Chemistry & Biology 13, 1265–1275, December 2006 DOI 10.1016/j.chembiol.2006.09.016

Targeting Glycosylation Pathways and the Cell Cycle: Sugar-Dependent Activity of Butyrate-Carbohydrate Cancer Prodrugs

Srinivasa-Gopalan Sampathkumar,[1] Mark B. Jones,[1] M. Adam Meledeo,[1] Christopher T. Campbell,[1] Sean S. Choi,[1] Kaoru Hida,[1] Prasra Gomutputra,[1] Anthony Sheh,[1] Tim Gilmartin,[2] Steven R. Head,[2] and Kevin J. Yarema[1,*]
[1]Whiting School of Engineering
Clark Hall 106A
Johns Hopkins University
3400 North Charles Street
Baltimore, Maryland 21218
[2]DNA Microarray Core Facility
The Scripps Research Institute
La Jolla, California 92037

Summary

Short-chain fatty acid (SCFA)-carbohydrate hybrid molecules that target both histone deacetylation and glycosylation pathways to achieve sugar-dependent activity against cancer cells are described in this article. Specifically, *n*-butyrate esters of *N*-acetyl-D-mannosamine ($But_4ManNAc$, 1) induced apoptosis, whereas corresponding *N*-acetyl-D-glucosamine ($But_4GlcNAc$, 2), D-mannose (But_5Man, 3), or glycerol (tributryin, 4) derivatives only provided transient cell cycle arrest. Western blots, reporter gene assays, and cell cycle analysis established that *n*-butyrate, when delivered to cells via any carbohydrate scaffold, functioned as a histone deacetylase inhibitor (HDACi), upregulated $p21^{WAF1/Cip1}$ expression, and inhibited proliferation. However, only 1, a compound that primed sialic acid biosynthesis and modulated the expression of a different set of genes compared to 3, ultimately killed the cells. These results demonstrate that the biological activity of butyrate can be tuned by sugars to improve its anticancer properties.

Introduction

This article describes compounds that target two hallmarks of cancer: the loss of cell cycle checkpoint control [1] and abnormal glycosylation [2, 3]. Uncontrolled cell proliferation characteristic of transformed cells is, in part, epigenetic in origin, and results from cancer-specific anomalies in chromatin structure [4, 5]. Chromatin consists of DNA, histones, and accessory proteins, such as histone deacetylase (HDAC) and histone acetyltransferase (HAT). Together, HDAC and HAT remodel chromatin to provide a "code" recognized by nonhistone proteins that regulate gene expression [4]. Not surprisingly, there is intense interest in the precise mechanisms that regulate chromatin remodeling, with the bulk of these efforts focused on the inhibition of HDACs. In recent years, the ability of HDAC inhibitors (HDACi) to disrupt cell cycle progression or selectively induce apoptosis via derepression of genes, such as P21 and BAX, in cancer cells has made HDAC inhibition an attractive avenue for the development of anticancer drugs [6–8].

n-Butyrate, a naturally-occurring HDACi belonging to the class of compounds known as short-chain fatty acids (SCFAs) [9], has selective activity toward transformed cells compared with healthy cells [10]. Efforts to exploit *n*-butyrate for clinical treatment of cancer, however, have been stymied by its poor pharmacological properties and the high concentrations (up to 50 mM) needed for bioactivity [11]. One approach to avoid the pharmacokinetic limitations of *n*-butyrate has been to use traditional enzyme-substrate screening assays to discover "drug-like" small-molecule HDACi, such as trichostatin, suberoylanilide hydroxamic acid (SAHA), and MS-275, among others [7]. These compounds inhibit cell growth, induce terminal differentiation, and prevent tumor formation in animal models [12]. Despite these attractive anticancer properties and nanomolar binding affinities when tested against purified enzyme, the majority of current HDACi clinical candidates require unrealistically high (up to millimolar) concentrations to be effective against cells [4].

A strategy to improve the pharmacological properties of HDACi has been to structurally modify *n*-butyrate to increase cellular uptake. A prominent example of this approach is 4-phenylbutyrate (4PB), which is an FDA-approved (albeit for urea cycle disorders, not cancer [13, 14]) and "generally well tolerated" derivative of *n*-butyrate [15]. Despite the relative safety of 4PB, secondary metabolites [16] and a relatively modest gain in efficiency (~2- to 10-fold) reduce prospects for its clinical application. In another approach, *n*-butyrate is delivered in the form of prodrugs as an arginine salt or as esters of lactic acid and cholesterol to enhance cellular uptake and retention. Perhaps the most successful compound where *n*-butyrate is delivered as a monovalent ester has been pivaloyloxymethyl butyrate (Pivanex, or AN-9) [17], which showed modest efficacy against non-small cell lung cancer in Phase II trials [18].

Based on the enduring difficulties in supplying HDACi to cells at sufficiently high concentrations to support bioactivity, prodrugs have been studied where carbohydrate moieties function as multivalent "cores" for the simultaneous delivery of several *n*-butyrate molecules. Specific examples of *n*-butyrate delivered via sugar-appended esters include straight-chain threitol and tributyrin cores (glycerol tributyrate, 4) [19], as well as the cyclic scaffolds glucose [20], galactose, mannose, and xylitol [21, 22]. Over the past 2 decades, these strategies have shown sufficient promise in clinical tests to support continuing investigation, but a breakthrough justifying widespread clinical use remains elusive [6]. We reasoned that one factor hindering progress was that carbohydrate scaffolds have served only as innocuous delivery vehicles; by contrast, we proposed that by appropriate selection of the monosaccharide, the activity of *n*-butyrate could be augmented through glycosylation pathways.

Although glycosylation-based therapies for cancer have been slow to emerge, growing evidence of the

*Correspondence: kyarema1@jhu.edu

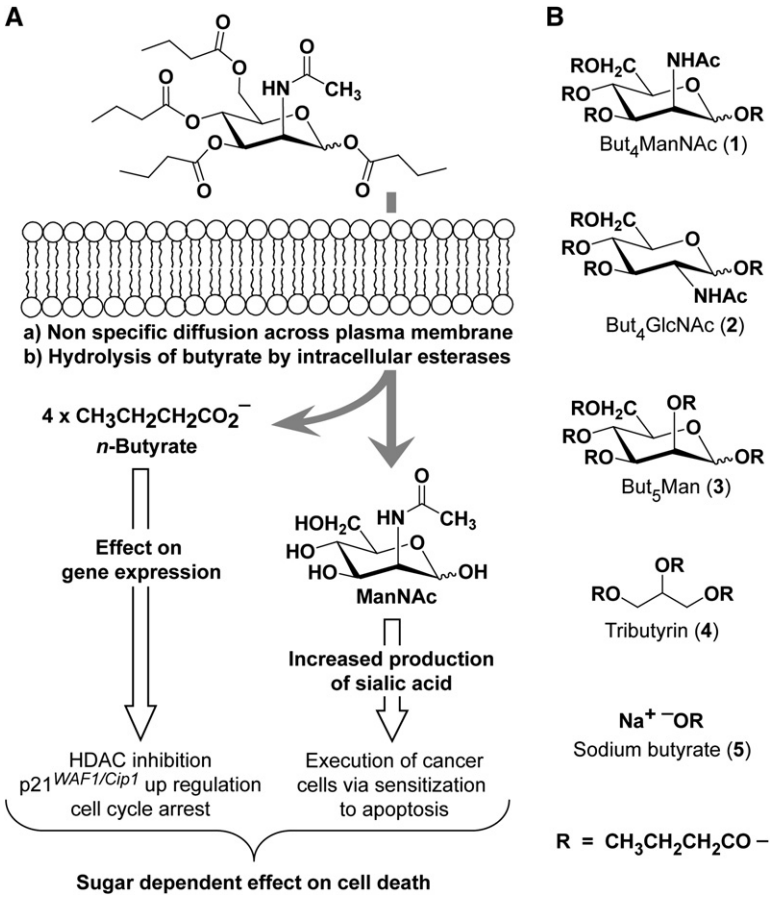

Figure 1. Sugar-Dependent Targeting of Glycosylation and Cell Cycle Progression

(A) Schematic diagram showing the cellular uptake of **1**, intracellular release of butyrate and ManNAc, and the sialic acid biosynthetic pathway related activity resulting in cell cycle arrest and apoptosis.

(B) Structures of butyrate-carbohydrate hybrid compounds studied in this report.

many roles of sugars in the carcinogenic transformation of cells [23, 24] has established oligosaccharide pathways as a rich and largely untapped opportunity to improve cancer treatments [3, 25, 26]. Although nascent efforts are under way to develop cancer vaccines and immunotherapies [27, 28] based on glycoconjugate structures used as biomarkers to distinguish cancer cells from their healthy counterparts [24, 29], actual intervention in the biochemical pathways responsible for cancer-specific glycosylation defects is almost nonexistent. The strategy of using a sugar as a delivery vehicle for HDACi, however, opens the door for targeting glycosylation pathways. In particular, we reasoned that the hexosamines (6-carbon amino sugars) that cells employ for building the oligosaccharides [30] that characterize both healthy and diseased cells and exert influence over cell signaling pathways involved in cancer [31] could be modulated to influence the activity of butyrate.

There are three predominant hexosamines in human cells, and each is relevant to cancer biology. First, *N*-acetylglucosamine (GlcNAc) forms the anchoring residues for *N*-linked oligosaccharides, which are often aberrantly displayed on cancer cells [29]. GlcNAc also plays a second, intracellular role in cancer through the addition and removal of *O*-GlcNAc on oncoproteins, tumor suppressors, and other proteins involved in the pathogenesis of tumors [32]. Second, *N*-acetylgalactosamine (GalNAc) is the chain initiator for *O*-glycosylated proteins, and aberrant *O*-glycan chains found in cancer often expose previously masked glycans or peptide motifs as new antigenic targets [31], such as mucins [33, 34]. Finally, a third hexosamine tied to cancer is *N*-acetylmannosamine (ManNAc); this sugar is the focus of this study and illustrates the value of considering carbohydrate expression while designing drugs for cancer treatment.

ManNAc has several attractive features that led us to select it as the lead hexosamine for drug development. First, it is a committed precursor for the sialic acid biosynthetic pathway, thus enabling the targeting of a single biochemical pathway [35, 36]. Second, by altering flux through the sialic acid biosynthetic pathway [37], ManNAc changes sialyltransferase and sialidase activity [38] and alters the display of sialic acid on cell surface glycoproteins [39, 40] and glycolipids [41, 42]. Because sialoglycans modulate apoptosis [39–43], we reasoned that the cell cycle inhibitory properties of *n*-butyrate could be enhanced in combination with changes to sialic acid metabolism (Figure 1A) by using the hybrid molecule, But$_4$ManNAc (**1**, Figure 1B), known to efficiently increase sialic acid production in cells [44]. In this article, we show that butyrate gains a unique ability to induce apoptosis when presented to cells as **1**, and demonstrate that **1** has characteristic SCFA activity and activates sialic acid biosynthesis, as expected, due to its butyrate and ManNAc components, respectively. In control experiments, delivery of *n*-butyrate via other carbohydrate scaffolds only gave transient growth inhibition, illustrating the necessity of targeting a specific glycosylation pathway—in this case, sialic acid biosynthesis—to achieve the desired sugar-dependent activity.

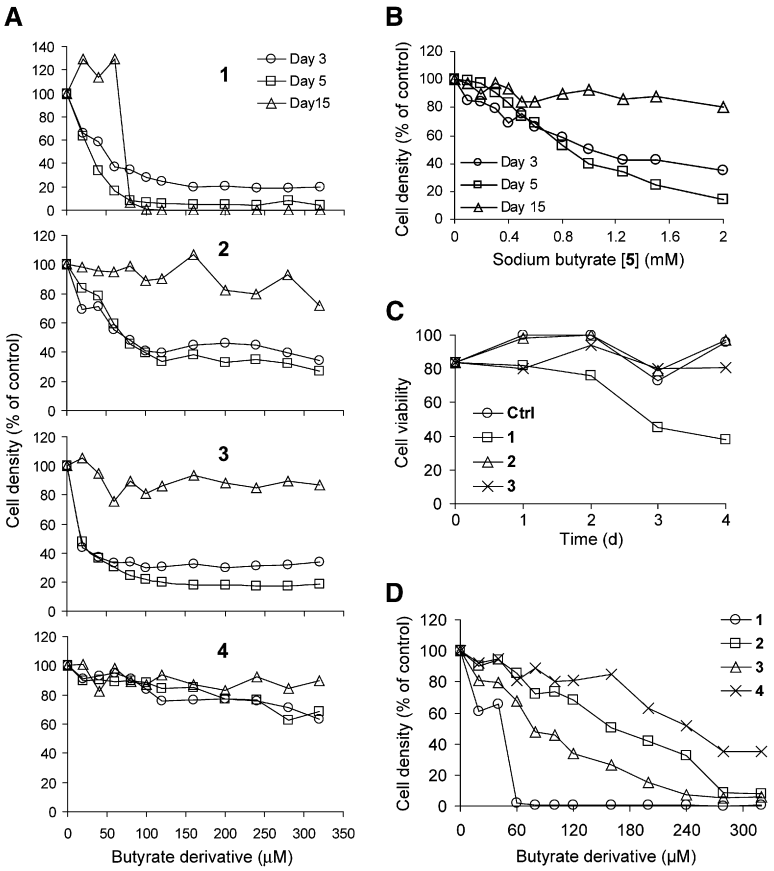

Figure 2. Arrest and Execution of Cancer Cells by Compound **1**, $But_4ManNAc$

(A) Short-term (Days 3 and 5) and long-term (Day 15) growth characteristics of Jurkat cells incubated with **1–4**; treatment with **1** induces both growth arrest and cell death, whereas cells treated with either **2**, **3**, or **4** resumed cell growth over the long term.

(B) Growth characteristics of Jurkat cells incubated with **5**.

(C) Trypan blue cell viability assay of Jurkat cells incubated with **1–3** at 200 μM.

(D) Effect of **1–4** on growth characteristics of HL-60 cells on Day 15. Standard deviations of three replicate experiments were less than 10%, and the error bars were omitted for clarity.

Importantly, the full effects of **1** could not be reproduced by concurrently delivering butyrate and ManNAc as separate molecules, indicating that the hybrid molecules are critical for achieving the novel bioactivities described here.

Results and Discussion

Butyrate-Induced Cell Death Is Dependent on the Core Sugar Moiety

To test the hypothesis that monosaccharides tune the activity of butyrate, perbutyrate derivatives of *N*-acetyl-D-mannosamine ($But_4ManNAc$, **1**, Figure 1B) and two control monosaccharides (*N*-acetyl-D-glucosamine [$But_4GlcNAc$, **2**] and D-mannose [But_5Man, **3**]) were synthesized (see the Supplemental Data available with this article online) and tested on human cancer cells. To briefly explain the rationale for the controls, **2** is the C2 epimer of **1** that, if anything, should be protective via the *O*-GlcNAc protein modification antistress mechanism [45], and **3** is the oxygen analog of **1** (i.e., it has an −OH group in place of the *N*-acetyl group at C2) that does not enter the sialic acid pathway. Finally, tributyrin (**4**) and sodium *n*-butyrate (**5**), compounds that have already undergone clinical evaluation [19], provided benchmarks for SCFA-based HDACi activity.

In initial assays, Jurkat (human T lymphoma) cells were incubated with **1–5**, and growth rates were monitored. As expected from the ability of butyrate to arrest cell cycle progression, reduced proliferation occurred when cells were incubated with **1–3** for 3–5 days (Figure 2A), while **4** and **5** showed minimal inhibition under the same conditions (Figures 2A and 2B). Despite similar cell counts at days 3 and 5 for **1–3**, trypan blue assays hinted that the underlying biological response to these compounds was different, as **1**, but not **2** or **3**, led to reduced cell viability (Figure 2C). Continued incubation amplified the early differences in cell viability, as, by day 15, cells treated with **2–5** resumed robust growth, whereas cells died when treated with **1** at concentrations $\geq$ 70–80 μM. These results indicated that cell cycle arrest induced by **2–4** up to 320 μM, and by **5** up to 2.0 mM, is transient. By contrast, for **1**, the core carbohydrate, ManNAc, played a crucial role in preventing long-term growth recovery and ensuring cell death. To test whether the sugar-dependent effects between ManNAc and *n*-butyrate were general toward cancer cells, **1–4** were evaluated in several human lines, with similar results (representative data, for the HL-60 line, are given in Figure 2D).

Hexosamine-Delivered Butyrate Has Characteristic SCFA Activity

In this article, we provide experimental evidence that the bioactivity supported by **1**, in particular, its unique ability to "arrest and execute" cells (Figures 1A and 2A), results from the cooperative effects of *n*-butyrate groups (which function as HDACi to provide growth arrest) and ManNAc (which activates the sialic acid pathway to induce apoptosis). First, we present evidence that **1** is an efficient delivery agent for biologically active butyrate. Based on seminal reports that butyrate induces

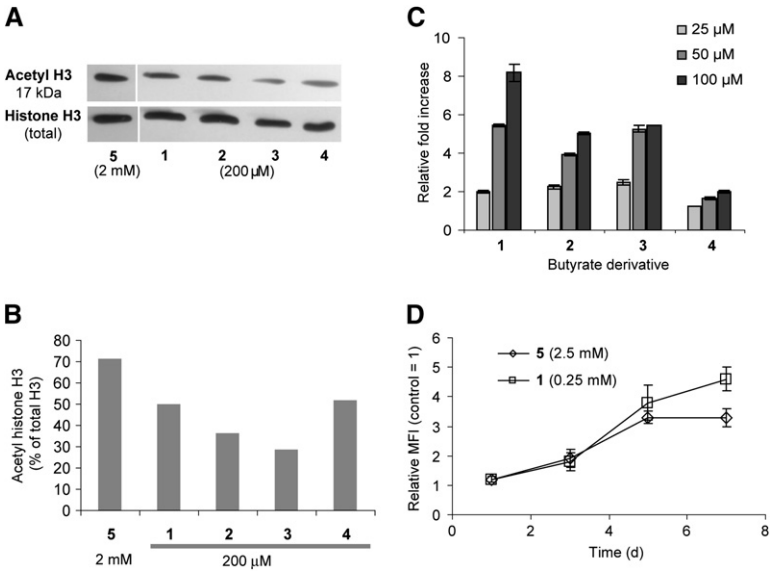

Figure 3. Upregulation of p21$^{WAF1/Cip1}$ by **1–5**

(A) SDS-PAGE showing the levels of acetylated histone H3 and total histone H3 in HeLa cells treated with **1–5** for 5 days. Two independent gels showed similar effects on the levels of histone H3 acetylation.

(B) Quantitation of levels of acetyl-histone H3 given as a percentage of total histone H3 quantified by densitometry using NIH ImageJ. Two replicate gels gave similar results.

(C) Expression of p21$^{WAF1/Cip1}$ promoter-driven luciferase in AD293 (HEK) cells transiently transfected with luc-p21$^{WAF1/Cip1}$ plasmid and subsequently incubated with **1–4**, as measured by luminometry. Error bars are standard deviation of the mean of at least three replicates.

(D) A time course of the endogenous expression of p21$^{WAF1/Cip1}$ in Jurkat cells treated with **1** or **5** using an anti-p21$^{WAF1/Cip1}$ antibody and flow cytometry quantification. Error bars represent standard deviation of the mean of at least three replicates.

differentiation of cancer cells with distinctive morphological changes [46], we verified the ability of **1** to induce similar effects in HeLa and AD293 (human embryonic kidney [HEK]) cells (Figure S1). Next, we used a set of three complementary assays, western analysis of histone acetylation, activation of gene expression measured by upregulation of exogenous and endogenous p21$^{WAF1/Cip1}$, and analysis of cell cycle progression, to prove that *n*-butyrate-sugar hybrids exhibit characteristic SCFA bioactivity.

Based on the precedent provided by per-acetylated saccharides [37, 47], we anticipated that **1–4** would have high membrane permeability and efficiently release *n*-butyrate inside a cell upon hydrolysis by nonspecific esterases. As a first step to test whether the sugar-supplied *n*-butyrate had characteristic SCFA activity, we monitored the acetylation of histone H3 in HeLa cells incubated with **1–4** by western blotting [48]. As a positive control for HDACi activity, incubation of cells with **5** at 2.0 mM showed relatively high levels of acetyl histone H3 (71% of total H3; Figures 3A and 3B). Evaluation of **1–4** at 200 μM led to relative acetylation levels of 50%, 36%, 29%, and 52% for **1**, **2**, **3**, and **4**, respectively (Figures 3A and 3B), verifying that biologically active butyrate is released intracellularly. Interestingly, **1** was a more effective inhibitor than **2** and **3**, a result that held in the next set of assays described below, testing p21$^{WAF1/Cip1}$ expression; by contrast, **1** and **4** inhibited histone deacetylation about equally, but the latter compound was significantly less efficient at activating p21$^{WAF1/Cip1}$ expression.

A consequence of HDAC inhibition, a hallmark of *n*-butyrate activity, is the upregulation of cell cycle checkpoint proteins, such as p21$^{WAF1/Cip1}$. When we evaluated luciferase activity from a luc-p21$^{WAF1/cip1}$ reporter plasmid [49] in HEK AD293 cells [50] exposed to **1–4**, expression increased in a dose-dependent manner (Figure 3C), with **1** showing higher activity than **2–4**. Interestingly, the activity of **4** was considerably lower than the activity of **1**, a result that does not correspond to the histone acetylation results where **1** and **4** had similar inhibition; this result, combined with the lack of toxicity for **4** (Figure 2A), clearly indicates that the ManNAc core of **1** contributed to the bioactivity of this compound by enhancing the effects of *n*-butyrate. To test whether p21$^{WAF1/Cip1}$-promoter activation held across cell lines and for endogenous p21$^{WAF1/Cip1}$, p21 levels were evaluated by flow cytometry [51] in Jurkat cells, and were found to increase in cells treated with both **1** and **5** (Figure 3D). Of practical importance for drug development efforts, endogenous p21$^{WAF1/Cip1}$ gene activation was achieved at considerably (~10×) lower concentrations for **1** than for **5** (Figure 3D).

Having confirmed that **1–5** activated p21$^{WAF1/Cip1}$-driven gene expression consistent with the known activity of SCFAs, we next tested whether these compounds also blocked cell cycle progression at the G2/M (4*n*) stage [52]. Standard propidium iodide (PI)/ribonuclease A (RNase A) assays [53] in asynchronous Jurkat cells showed that cell accumulation at the G2/M stage occurred after incubation with **2–4** (5 days, 200 μM) without measurable apoptosis (Figure 4A). In contrast, the majority of cells treated with **1** appeared to be apoptotic (< 2*n*), with very few remaining at the G0/G1 (2*n*) stage. At lower concentrations (0–75 μM), however, **1** supported a stepwise decrease in G0/G1 accumulation, with a concomitant increase in cells at the G2/M stage, consistent with known ability of butyrate to arrest cell cycle progression (Figure 4B). Nonviable cells (sub-G0) accumulated when concentrations of **1** exceeded 75 μM, the concentration required for cell death after 15 days of exposure (Figure 2A).

A time- and concentration-dependent comparison of Jurkat cells treated with **1** provided results (Figure 5) consistent with the growth inhibition and trypan blue toxicity data presented earlier (in Figure 2C). Control cells showed little change in cell cycle status up to day 4, after which a minor increase in cells at the G0/G1 stage was seen due to growth saturation that occurred upon reaching a density of > 2.0 × 10^6 cells/ml (Figure 5A). Upon treatment with 100 μM of **1** (Figure 5B), there was strong cell cycle inhibition at the

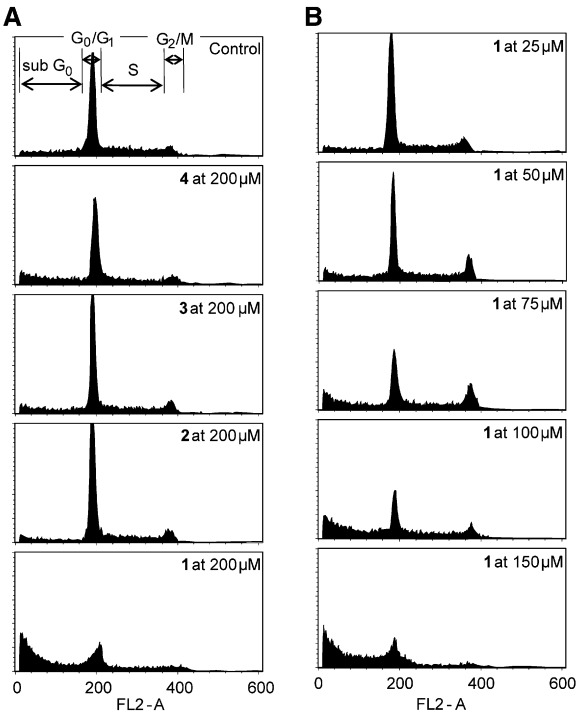

Figure 4. Cell Cycle Arrest and Apoptosis

(A) Flow cytometry histograms showing DNA content and cell cycle status of Jurkat cells incubated with 1–4 at 200 μM for 5 days measured by PI/RNase A staining.

(B) DNA content of Jurkat cells incubated with 1 at 25–150 μM, for 5 days, showing a dose-dependent increase in the population of apoptotic cells.

G2/M stage that was sustained until day 6, along with an increasing number of cells with less than 2*n* (i.e., fragmented) DNA. At 200 μM (Figure 5C), cells accumulated rapidly at the G2/M stage, with a concomitant decrease in the G0/G1 stage. Significantly, by day 4, a substantial proportion of the cells showed DNA in the sub-G0 range; by day 6, this response was almost complete. DNA fragmentation in the sub-G0 range is consistent with chromosomal degradation that occurs in apoptosis; therefore, the sub-G0 accumulation seen here upon treatment with **1**, combined with our previous extensive characterization of ManNAc analog-induced apoptosis in Jurkat cells [44, 54], strongly indicated that this compound killed cells through an apoptotic mechanism. Nonetheless, to obtain direct evidence of apoptosis, we measured caspase-3 activity [44] in Jurkat cells incubated with 25, 50, and 100 μM of **1** for 48 hr, and found increases of ~4-, 8-, and 14-fold, respectively (Figure S2).

The Unique Activity of 1 Cannot Be Reproduced by Its ManNAc and *n*-Butyrate Components

The results of the toxicity assays, western blotting, $p21^{WAF1/cip1}$ expression, and cell cycle studies reported above established that **1** was an efficient delivery vehicle for introducing biologically active *n*-butyrate into cells, and had a unique ability to induce apoptosis. We were interested in exploring whether the advantages of **1** simply resulted from this compound acting as a better delivery agent for *n*-butyrate than the other derivatives; this possibility was suggested by the luciferase reporter assay data (Figure 3A), where **1** had ~50% higher activity at 100 μM than **2** or **3**. This result was counterintuitive, because **3** delivered five butyrate equivalents into a cell, whereas **1** only delivered four. One—albeit unlikely—possibility to explain this result was that ManNAc increased the efficiency of butyrate through mechanisms unrelated to its direct attachment to this SCFA via ester linkages; for example, through an allosteric increase in membrane transport activity. In order to discount such a possibility, we tested luc-$p21^{WAF1/\ Cip1}$ expression after incubating cells with a mixture of free monosaccharide form of ManNAc and **5** in a 1:4 ratio designed to mimic the relative molar ratios of the sugar and butyrate moieties in **1**. The supplementation of **5** with ManNAc had no effect on luciferase activity, which required millimolar concentrations of each compound (Figure 6A), indicating that the ability of **1** to activate butyrate-specific gene expression patterns at micromolar concentrations was contingent upon supplying the sugar and SCFA functionalities in the same molecule.

A clue for the unique ability of **1** to induce apoptosis emerged from a comparison of the toxicity data for cells treated with **1–3** with the results of the luciferase reporter gene assay. Specifically, at 50 μM and below, none of these three compounds were toxic after 15 days (Figures 2A–2C), and they all showed similar activation of $p21^{WAF1/Cip1}$ expression (Figure 3C) in this concentration range. Interestingly, gene activation for **1** continued to increase significantly between 50 and 100 μM for **1**, whereas the corresponding increase was slight for **2** or **3**; importantly, apoptosis associated with **1** (Figure 2A) also occurred over this concentration range, suggesting that a threshold of $p21^{WAF/Cip1}$ activation—not reached by **2** or **3** (Figure 3C)—may be required for toxicity. Another nonexclusive possibility was that the *n*-butyrate-specific effects of **1** were augmented by the ability of this compound to support a rapid increase in sialic acid biosynthesis, which once again occurred over the same range of concentrations (Figure 6B).

The data discussed in the previous paragraph illustrates that **1** serves the dual role of functioning as an efficient delivery vehicle for butyrate, evidenced by $p21^{WAF1/Cip1}$ activation (Figure 6A), and for ManNAc, as shown for sialic acid production (Figure 6B). In both cases, the biological response to **1** took place at much lower concentrations than when ManNAc and **5** were concurrently added to cells, but as separate compounds. These experiments, however, did not address whether supplying these compounds as separate molecules, albeit at higher concentrations, could enhance apoptosis. This possibility was raised by studies in which HDACi have been combined with a second drug to augment their anticancer activity [55]. Accordingly, we tested whether ManNAc, presumably through its primary metabolic fate of increasing flux into the sialic acid pathway, could similarly complement the activity of butyrate by sensitizing cells to its effects. To this end, Jurkat cells were incubated with 50 and 100 mM ManNAc for 48 hr, which increased total levels of sialic acid by ~7- and 9-fold, respectively, compared with

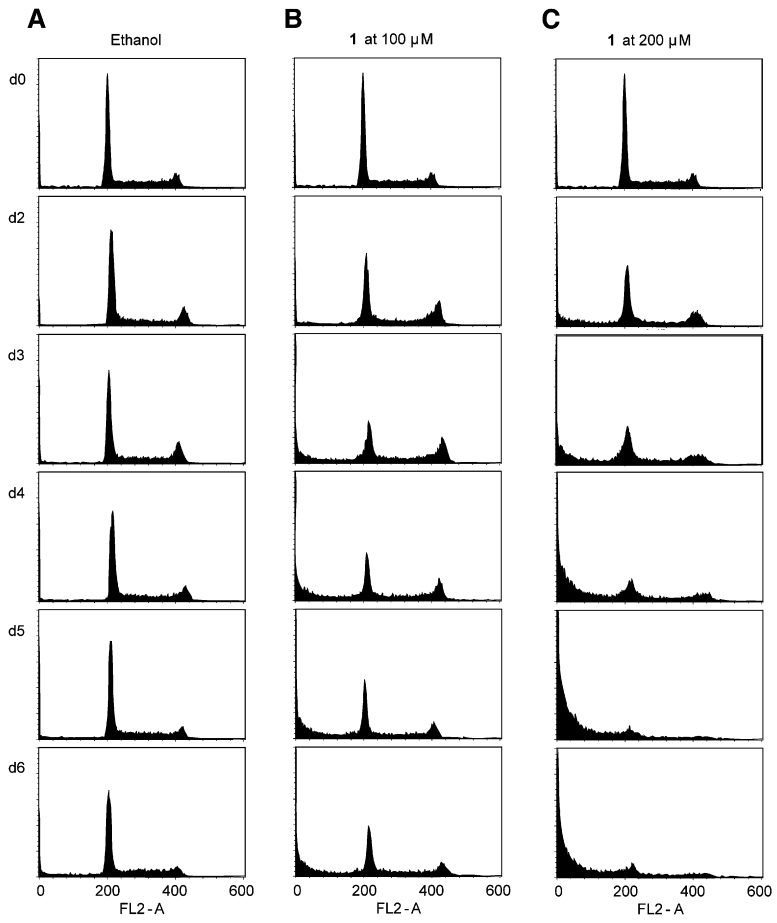

Figure 5. Time Course of Cell Cycle Arrest and Cell Death

(A) Flow cytometry histograms showing DNA content and change in cell cycle status of Jurkat cells over a 6 day period.

(B) DNA content and cell cycle status of Jurkat cells incubated with **1** at 100 μM.

(C) DNA content and cell cycle status of Jurkat cells incubated with **1** at 200 μM.

untreated controls (Figure 6C). The test cells were then exposed to **5**, and their growth was quantified by cell counting after 5 days (Figure 6D). The proliferation of ManNAc-treated cells was inhibited modestly, but in a statistically significant manner, at concentrations of **5** below 0.5 mM compared with untreated control cells (Figure 6E). Upon continued incubation, both the control and ManNAc-treated cells exposed to 1.5 mM and lower concentrations of **5** recovered and resumed robust growth by Day 15. The ManNAc-treated cells, however, showed increased susceptibility to **5** at 2.0 mM compared to the controls (Figure 6F; there was significant toxicity for all samples when treated with **5** at concentrations higher than 2.5 mM).

The sensitization of cells pretreated with ManNAc to the effects of butyrate highlighted two important features of the strategy exemplified by **1** of using sugar-SCFA hybrid molecules as anti-cancer agents. First, on a conceptual level, these results provide experimental support for the hypothesis that glycosylation pathways (shown by the activation of sialic acid biosynthesis) can be exploited to complement the activity of butyrate. Second, on a practical level, the levels of butyrate (2.0 mM) and ManNAc (50–100 mM) required for even modest growth inhibition (Figure 6E) and toxicity (Figure 6F), when used separately, exceed realistic drug development parameters. The necessity for combining ManNAc and **5** into a single molecule was reinforced by the inability of ManNAc to alter cell cycle status at 10 mM (Figure 6G, top panel). Similarly, the more pharmacologically realistic level of ManNAc of 125 μM failed to augment the activity of **5** (Figure 6G, center panels). By contrast, almost complete DNA fragmentation, which is indicative of apoptosis, resulted from 100 μM of **1** (Figure 6G, bottom panel).

To recap the inability of the combined administration of ManNAc and **5** to phenocopy the effects of **1**, we briefly revisit the data presented in Figure 6B. In this experiment, a combination of ManNAc and **5** in the 1:4 ratio found in **1** did not result in an increase in sialic acid production up to the dose-limiting level of a mixture of 5.0 mM ManNAc and 20 mM of **5**. ManNAc by itself resulted in a dose-dependent increase in sialic acid production between 0.2 and 100 mM to a maximum of $\sim 2.0 \times 10^{10}$ molecules/cell. By contrast, sialic acid production for cells treated with **1** occurred at much lower concentrations (between 25 and 100 μM), and reached double ($>4.0 \times 10^{10}$ molecules/cell) the level achieved with ManNAc. Importantly, the level of sialic acid produced in cells treated with ~ 75 μM of **1**, the concentration required for toxicity (Figure 2A), was $\sim 4.0 \times 10^{10}$ molecules/cell. As a result, the free monosaccharide form of ManNAc leaves a significant shortfall (indicated by the asterisk in Figure 6B) in the amount of sialic acid produced compared with cells experiencing the full toxic effects of **1**. Consequently, it is not surprising that efforts to reproduce the cellular response to this compound, with its two component moieties, ManNAc

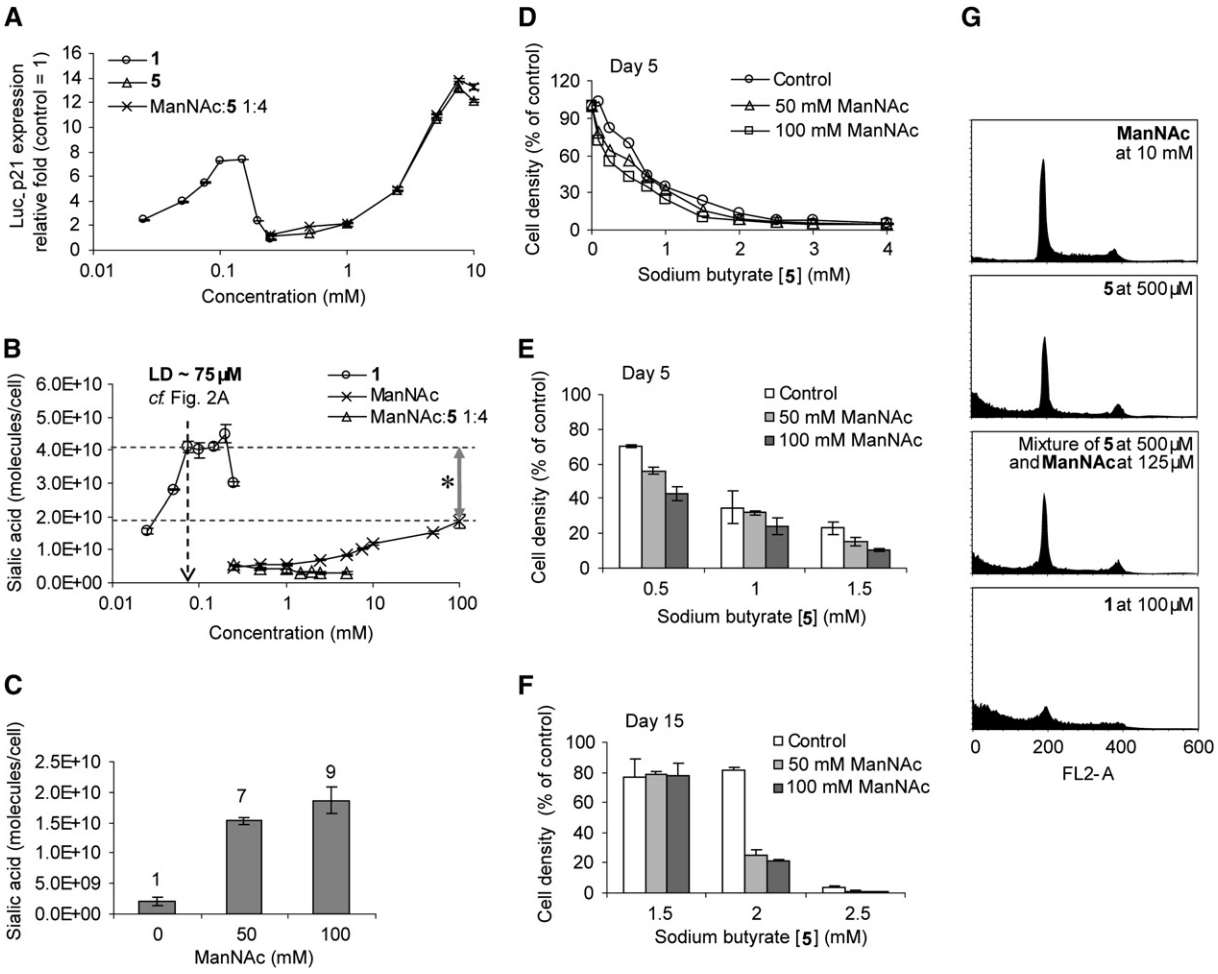

Figure 6. Comparisons of ManNAc and *n*-Butyrate as the Hybrid Molecule **1** or as Single Molecular Entities Added to Cells in Combination

(A) Comparison of luc-p21$^{WAF1/Cip1}$ expression in AD293 (HEK) cells treated with either **1** (0–250 μM) or **5** (0–10 mM) alone, or a mixture of **5** (0–10 mM) and ManNAc (0–2.5 mM) at a relative molar ratio of 4:1. In this set of assays, concentrations of the test compounds were increased until signal-limiting toxicity occurred. Error bars represent standard deviation of at least three replicate samples.

(B) Total sialic acid content, determined by periodate-resorcinol assay [63], in Jurkat cells incubated with either **1** (0–250 μM) or ManNAc (0–100 mM) alone, or a mixture of ManNAc (0–5 mM) and **5** (0–20 mM) at a molar ratio of 1:4.

(C) Total sialic acid content in Jurkat cells primed for increased sialic acid production by incubation with 0, 50, and 100 mM of ManNAc for 48 hr.

(D) Short-term growth characteristics of Jurkat cells preincubated with 50 or 100 mM ManNAc, or without ManNAc, for 48 hr, and then cultured in the presence of **5** at 0–4.0 mM after 5 days. Error bars are omitted for clarity; the standard deviation (SD) of the mean is less than 5 % for three replicates.

(E) Short-term growth characteristics of Jurkat cells on Day 5 (highlight of the data in Figure 6D) at 0.5, 1.0, and 1.5 mM of **5**. Error bars represent SD of at least two replicate samples.

(F) Long-term growth characteristics of Jurkat cells preincubated with ManNAc at 50 or 100 mM, or without ManNAc, for 48 hr, and then cultured in the presence of **5** at 0–4.0 mM for 15 days. Cell densities at 1.5, 2.0, and 2.5 mM are shown. Error bars represent SD of at least two replicate samples.

(G) Comparison of the effect of ManNAc, **5**, a 4:1 molar mixture of **5** and ManNAc, or **1** on cell cycle and DNA fragmentation in Jurkat cells after 5 days of incubation studied by PI/RNase A staining.

and **5**, as shown in Figures 6C–6F, met with only modest success. When combined in the same molecule, however, the concentration range (50–100 μM) where **1** shows its full range of bioactivity (i.e., apoptosis, Figure 2A; p21$^{WAF1/Cip1}$ activation, Figures 3C and 6A; and sialic acid production, Figure 6B) compares favorably with other SCFA-based drug candidates already under clinical evaluation, such as **4** [19] or synthetic molecules that include hydroxamates, cyclic peptides, aliphatic acids, and benzamides [4].

Mechanistic Connections between *n*-Butyrate, ManNAc, and the Unique Activity of 1

Having established that ManNAc and *n*-butyrate must be delivered together as a single hybrid molecule to support the robust activation of sialic acid biosynthesis associated with apoptosis, we turned our efforts toward uncovering mechanistic clues to explain how the sugar moiety generates the unique cellular responses observed for **1**. Several factors indicate that sialic acid is involved in mediating the unique biological effects of **1**. First, the data

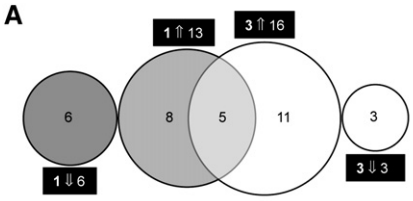

B

Up regulated by **1** (13 genes)

Amphiregulin (schwannoma-derived GF)
Bamacan
BMP 2 Long transcript
BMP 6 precursor
BMP 2 Short transcript
CCL-26 (Eotaxin-3)
EXTL2 [GAG enzyme]
Fucose-1-phosphate guanyltransferase
Interleukin 8
Interleukin 1, beta
Melanoma cell adhesion molecule, Short transcript
NJAC protein
PPL13 (LGALS14)

Down regulated by **1** (six genes)

Galectin 12 (long variant)
Galectin 12 (short variant)
Galectin-related inhibitor of proliferation isoform b
Interferon induced transmembrane protein 1 (9-27)
Interferon gamma-induced precursor
MUC1, transmembrane

C

Upregulated by **3** (16 genes)

Amphiregulin (schwannoma-derived GF)
BMP 2 Long transcript
CCL-26 (Eotaxin-3)
gp130-RAPS
GRO1 oncogene
Interleukin 8
Interleukin 1, beta
Interleukin 6 signal transducer sequence A
Interleukin 6 signal transducer sequence B
Manic fringe (Drosohila) homolog - Short Trans
Macrophage stimulating 1 (hepatocyte growth factor-like)
Notch3 - Long Trans
PSGL-1 (selectin P ligand)
Secreted frizzled-related protein 1
Similar to glucosamine-phosphate N-acetyltransferase - short
TGF, beta receptor III

Down regulated by **3** (three genes)

FGF 4
follistatin isoform FST317 precursor
Leptin receptor

Figure 7. GLYCOv3 Microarray Analysis of the Effect of **1** and **3** on Gene Expression of Glycan Binding Proteins

(A) The numbers of genes up- or down-regulated by 2-fold or higher in MDA-MB-231 cells incubated with **1** or **3** at 125 μM for 3 days relative to ethanol-treated controls are shown in Venn diagrams. Expression data were obtained with the GLYCOv3 gene chip array that contains probe sets to monitor the expression of approximately 2000 human and mouse transcripts relevant to glycosylation.

(B) List of genes up- or down-regulated by **1** by at least 2-fold.

(C) List of genes up- or down-regulated by **3** by at least 2-fold. The overlapping changes in gene expression by **1** and **3** are given in bold.

presented in Figure 6 experimentally links the production of sialic acid with sensitization of cells to butyrate. Second, ManNAc has been described as being a dedicated metabolic precursor to the biosynthesis of sialic acid, with only one report describing a different biological fate for this sugar; the one situation where ManNAc is not used for sialic acid biosynthesis is that in which the renin binding protein (RBP), which also holds epimerase activity, converts ManNAc to GlcNAc [56]. This alternate metabolic route for ManNAc did not apply to the current studies, because RBP is not expressed in Jurkat cells [56] and, even if it were, the control experiments done using **2** eliminated the possibility that the combination of butyrate and GlcNAc could reproduce the effects of **1**. Finally, a solid body of literature has emerged implicating sialic acid and its modifications in several facets of the apoptotic response [39–43], and it is reasonable that the high levels of this sugar produced in cells at concentrations of **1** associated with apoptosis (Figure 6B) can interfere with this complex regulatory system.

Despite this compelling indirect evidence, it will be challenging to provide unequivocal proof for the role of sialic acid in mediating the biological effects of **1**. First, the obvious explanation—that sialic acid has a direct effect on the genes involved in sialic acid metabolism—has been ruled out by quantitative real-time PCR analysis of ManNAc-treated cells [57]. Second, attempts to mimic the unique effects of **1** using a 4:1 molar mixture of **5** and ManNAc are hampered by the limited cellular uptake of this sugar; consequently, it is not possible to attain the high levels of sialic acid associated with the toxicity of **1** with the free monosaccharide form of ManNAc (Figure 6). An alternative approach to mimic the effects of **1** by using Ac4ManNAc, which is known to increase total sialic acid to much higher levels than ManNAc (see [37] and Figure S3), to prime the sialic acid biosynthesis is not helpful in resolving the individual roles played by ManNAc and **5**, because the intracellularly released acetate (an SCFA in itself) affects the expression of sialic acid pathway genes (Figure S4 and accompanying discussion). As a result, the specific cellular effects arising from the high levels of sialic acid supported by **1** cannot be determined in the absence of *n*-butyrate or acetate. Aside from pharmacokinetic considerations, another issue is that the two components of **1** may interact by modulating the same molecules involved in apoptosis—for example, both sialic acid [39] and *n*-butyrate [58, 59] modulate the sensitivity of cancer cells to anti-Fas-mediated apoptosis.

Unraveling the specific contributions of butyrate to the overall activity of **1** is likely to be as complex as for sialic acid, and will require much work beyond the current report. However, as a clue to guide further investigation, and to emphasize the powerful ability of the core monosaccharide to modulate SCFA activity, we further investigated the repercussions—beyond the hallmark changes to $p21^{WAF1/Cip1}$ expression associated with SCFAs—of the differential effects of **1** and **3** on histone acetylation (Figure 3A). Following the strategy reported by Williams and coworkers to uncover the combined effects of *n*-butyrate and sulindac or cycloheximide by genomic analysis [60], we undertook a focused microarray study of glycan binding proteins (using the GLYCOv3 chip developed by The Consortium for Functional Glycomics [61]) on the effects of **1** and **3** compared to ethanol-treated controls in the human breast cancer MDA-MB-231 line. This experiment showed that, although a common set of genes was regulated by both compounds, consistent with the presence of the common moiety butyrate, there was considerable variation in the overall pattern of gene expression (Figure 7), thereby, once again, clearly illustrating the capacity of the core sugar to influence the overall cellular response to SCFAs.

In summary, notwithstanding the circumstantial but compelling evidence that the sugar-specific effects of **1** occur via a complex interplay involving sialic acid metabolism and the effects of butyrate on histone acetylation, other mechanistic explanations remain open. For example, currently unknown metabolic fates for ManNAc (other than the priming of sialic acid biosynthesis) may exist. Alternately, an intriguing possibility is that HDACi activity occurs before complete removal of *n*-butyrates from the sugar core structure. Then, based on the precedent of where *n*-butyrate, 4PB, and trichostatin have different activity profiles by virtue of the chemical context of the butyrate moiety itself [5], a partially butyrated derivative of mannose would be expected to have a different effect on gene expression compared with a partially butyrated derivative of ManNAc and, thereby, to account for the differences in gene expression between **1** and **3** (Figure 7).

Conclusions

Regardless of the precise mechanisms involved, the detailed elucidation of which is beyond the scope of this study, we have presented experimental evidence in support of the intriguing strategy that the HDACi activity of *n*-butyrate can be tuned by the monosaccharide core that was, in the past, only designed to be an innocuous delivery vehicle. Importantly, we showed that neither ManNAc nor *n*-butyrate, the constituent components of **1**, when supplied as separate molecules, could initiate apoptosis at therapeutically relevant concentrations. As such, this emphasizes the need to combine both functionalities in a single hybrid molecule. In conclusion, we believe that our approach of combining glycosylation with HDACi constitutes an important contribution to the recent flurry of butyrate-based anticancer research that has been compared to putting "old wine in new bottles" [62].

Significance

Loss of cell cycle checkpoint control and abnormal glycosylation are two of the major cellular aberrations associated with cancer. Multiple strategies to correct defects in cell cycle checkpoints arising from abnormal histone-chromatin interactions are now under investigation, including intense efforts to develop histone deacetylase inhibitors (HDACi), such as butyrate. By contrast, glycosylation-targeted cancer therapies have been slow to emerge. To meet this void, we synthesized butyrate-hexosamine hybrids that target both gene regulation and glycoconjugate expression and, by enhancing bioactivity by a sugar-dependent mechanism, ensure both the "arrest" and "execution" of cancer cells. Narrowly, this work provides a promising approach to complement the anticancer potential of butyrate; broadly, it provides a concrete example of bringing glycosylation-based therapies closer to reality.

Experimental Procedures

Cell Culture Methods and Supplementation with Butyrate Derivatives 1–5

For cell culture studies, But_4ManNAc (**1**) [44] was used as a mixture of anomers (α/β = 10/90), But_4GlcNAc (**2**) as pure α-anomer, and But_5Man (**3**) as pure β-anomer (the intracellular hydrolysis of butyrate esters makes the anomeric configuration less relevant in these studies, and we found similar cellular toxicity effects between the α- and β-anomers). Stock solutions of the analogs were made in ethanol at 10 and 50 mM. In the case of cells growing in suspension, the solutions of **1–4** (or an ethanol control at an equivalent volume) were coated onto dishes, and the ethanol was allowed to evaporate prior to the addition of cells. Unless otherwise noted, throughout this study, Jurkat cells (Clone E-6; ATCC, Manassas, VA) were cultured in RPMI 1640 medium supplemented with 300 mg/l glutamine, 5.0% fetal bovine serum (FBS; HyClone, Logan, Utah) and 1.0% of a 100× pen/strep (P/S) stock solution containing penicillin (100 units/ml) and streptomycin (100 μg/ml); HL-60 cells (ATCC) were cultured in RPMI 1640 medium supplemented with 10% FBS and pen/strep; and AD293 (HEK), HeLa, and MDA-MB-231 cells (Stratagene, La Jolla, CA) were grown in DMEM medium with 10% FBS and pen/strep. In all cases, cells were incubated at 37°C in a 5.0% CO_2, water-saturated environment. Cell counting was performed with a Beckman Coulter Z2 particle counter (Beckman Coulter, Fullerton, CA) and hemacytometer.

Toxicity and Growth Inhibition Assays

Solutions of the analogs in EtOH (10 mM stock) were coated onto 24-well plates at a range of concentrations from 0 to 320 μM, and ethanol was allowed to evaporate. Jurkat cells (1.0×10^5) in 0.5 ml of medium were added to each well on Day 0. On Days 3 and 5, fresh medium (1.0 ml) was added to each well, cell cultures were mixed by gentle pipetting, and 100 μl of cell suspension from each well was counted. On Days 7, 9, 11, 13, and 15, 1.0 ml of cell suspension was removed from each well after thorough mixing, and fresh medium (1.0 ml) was added. Cells counts from Days 3, 5, and 15 were plotted as a percentage of control.

Western Analysis of Histone H3 Acetylation

The acetylation of histone H3 was analyzed by western blotting. Briefly, 2.0×10^6 HeLa cells were plated in 10 ml of DMEM medium supplemented with 10% FBS and 1% P/S in 10 cm T.C. dishes. After 24 hr, the medium was changed, and the cells were treated with either 40 μl ethanol, **5** (to give a final concentration of 2.0 mM), or **1**, **2**, **3**, and **4** (200 μM). After 5 days, the cells were harvested using a cell scraper, washed with PBS (2 × 5.0 ml), resuspended in 400 μl lysis buffer (100 mM HEPES, 1.5 mM $MgCl_2$, 10 mM KCl, 0.5 mM DTT, 1.5 mM PMSF), treated with 100 μl 1.0 N hydrochloric acid, vortexed, and kept overnight at 2°C. The lysate was centrifuged at 11,000 × g at 4°C for 10 min, and the supernatant was collected carefully and stored at −80°C. Protein concentration was estimated using Coomassie plus reagent (Pierce, Rockford, IL). SDS-PAGE was performed on 18% gels (Ready Gel; Bio-Rad, Hercules, CA) with 10 μg of protein lysate, and blotted to nitrocellulose membrane. The membranes were stained with anti-histone H3 (total H3; mouse monoclonal IgG1k, Cat. No. 05-499, 1:500; Upstate, Lake Placid, NY) and anti-acetylhistone H3 (rabbit antiserum, Cat. No. 07-353, 1:1000; Upstate), detected using HRP-linked affinity-purified horse anti-mouse IgG (heavy and light chains [H&L], cat. no. 7076) and affinity-purified goat anti-rabbit IgG (H&L, cat. no. 7074, 1:20,000; Cell Signaling Technology, Inc., Danvers, MA), respectively, and enhanced chemiluminescence reagents (Supersignal West Dura Extended Duration substrate; Pierce). At least two replicate gels were performed, scanned, and the band density quantified using ImageJ (National Institutes of Health, Bethesda, MD), and the results presented as the ratio of acetylated histone H3 to total histone H3.

Assay for Total Sialic Acid Production

Jurkat cells (5.0×10^6 cells in 10 ml medium) were incubated with **1–5** at various concentrations. After 3 days, the cells (1.0×10^6 per sample) were lysed by three freeze-thaw cycles. The cell lysates were analyzed by using an adapted version of the periodate-resorcinol assay [37, 63], with the periodic acid oxidation step performed on ice for quantification of total (i.e., free monosaccharide plus glycoconjugate bound) sialic acid. For each assay, a standard curve was obtained using *N*-acetylneuraminic acid (Pfanstiehl, Waukegan, IL) for calibration.

Supplemental Data

Supplemental Data, including detailed experimental procedure for synthesis and characterization of **2** and **3**, trypan blue cell viability assay, effects of **1** and **5** on morphology of HeLa and AD293 (HEK) cells, Luc-p21$^{WAF1/Cip1}$ luciferase reporter gene assays, analysis of cell cycle status by flow cytometry, toxicity assays, data on caspase-3 activity assay in Jurkat cells for dose-dependent apoptosis induced by **1**, the and GLYCOv3 microarray analysis are available online at http://www.chembiol.com/cgi/content/full/13/12/1265/DC1/.

Acknowledgments

We are grateful to K. Konstantopoulos for flow cytometer access, B. Vogelstein (Johns Hopkins Medical Institute [JHMI]) for the kind gift of luc-p21$^{WAF1/Cip1}$ plasmid, R.E. McCarty for luminometer access, and L. Blosser (JHMI) for help with cell cycle studies. Funding was from the Arnold and Mabel Beckman Foundation, the National Institutes of Health (1R01CA112314-01A1), and the National Science Foundation (QSB-0425668). The Gene Microarray Core resources and collaborative efforts were provided by The Consortium for Functional Glycomics, funded by NIGMS-GM62116.

Received: April 6, 2006
Revised: September 26, 2006
Accepted: September 27, 2006
Published: December 22, 2006

References

1. Møller, M.B. (2003). Molecular control of the cell cycle in cancer: biological and clinical aspects. Dan. Med. Bull. *50*, 118–138.
2. Dube, D.H., and Bertozzi, C.R. (2005). Glycans in cancer and inflammation—potential for therapeutics and diagnostics. Nat. Rev. Drug Discov. *4*, 477–488.
3. Fuster, M.M., and Esko, J.D. (2005). The sweet and sour of cancer: glycans as novel therapeutic targets. Nat. Rev. Cancer *5*, 526–542.
4. Kelly, W.K., and Marks, P.A. (2005). Drug insight: histone deacetylase inhibitors—development of the new targeted anticancer agent suberoylanilide hydoxamic acid. Nat. Clin. Pract. Oncol. *2*, 150–157.
5. Davie, J.R. (2003). Inhibition of histone deacetylase activity by butyrate. J. Nutr. *133*, 2485S–2493S.
6. Dashwood, R.H., Myzak, M.C., and Ho, E. (2006). Dietary HDAC inhibitors: time to rethink weak ligands in cancer chemoprevention? Carcinogenesis *27*, 344–349.
7. Drummond, D.C., Noble, C.O., Kirpotin, D.B., Guo, Z., Scott, G.K., and Benz, C.C. (2005). Clinical development of histone deacetylase inhibitors as anticancer agents. Annu. Rev. Pharmacol. Toxicol. *45*, 495–528.
8. Monneret, C. (2005). Histone deacetylase inhibitors. Eur. J. Med. Chem. *40*, 1–13.
9. Miller, S.J. (2004). Cellular and physiological effects of short-chain fatty acids. Mini Rev. Med. Chem. *4*, 839–845.
10. Papeleu, P., Vanhaecke, T., Elaut, G., Vinken, M., Henkens, T., Snykers, S., and Rogiers, V. (2005). Differential effects of histone deacetylase inhibitors in tumor and normal cells—what is the toxicological relevance? Crit. Rev. Toxicol. *35*, 363–378.
11. Novogrodsky, A., Dvir, A., Ravid, A., Shkolnik, T., Stenzel, K.H., Rubin, A.L., and Zaizov, R. (1983). Effect of polar organic compounds on leukemic cells: butyrate-induced partial remission of acute myelogenous leukemia in a child. Cancer *51*, 9–14.
12. Finnin, M.S., Donigian, J.R., Cohen, A., Richon, V.M., Rifkind, R.A., Marks, P.A., Breslow, R., and Pavletich, N.P. (1999). Structures of a histone deacetylase homologue bound to the TSA and SAHA inhibitors. Nature *401*, 188–193.
13. Rubenstein, R.C., and Zeitlin, P.L. (1998). A pilot clinical trial of oral sodium 4-phenylbutyrate (Buphenyl) in deltaF508-homozygous cystic fibrosis patients: partial restoration of nasal epithelial CFTR function. Am. J. Respir. Crit. Care Med. *157*, 484–490.
14. Burlina, A.B., Ogier, H., Korall, H., and Trefz, F.K. (2001). Long-term treatment with sodium phenylbutyrate in ornithine transcarbamylase-deficient patients. Mol. Genet. Metab. *72*, 351–355.
15. Roomans, G.M. (2003). Pharmacological approaches to correcting the ion transport defect in cystic fibrosis. Am. J. Respir. Med. *2*, 413–431.
16. Kasumov, T., Brunengraber, L.L., Comte, B., Puchowicz, M.A., Jobbins, K., Thomas, K., David, F., Kinman, R., Wehrli, S., Dahms, W., et al. (2004). New secondary metabolites of phenylbutyrate in humans and rats. Drug Metab. Dispos. *32*, 10–19.
17. Patnaik, A., Rowinsky, E.K., Villalona, M.A., Hammond, L.A., Britten, C.D., Siu, L.L., Goetz, A., Felton, S.A., Burton, S., Valone, F.H., et al. (2002). A phase I study of pivaloyloxymethyl butyrate, a prodrug of the differentiating agent butyric acid, in patients with advanced solid malignancies. Clin. Cancer Res. *8*, 2142–2148.
18. Reid, T., Valone, F.H., Lipera, W., Irwin, D., Paroly, W., Natale, R., Sreedharan, S., Keer, H., Lum, B., Scappaticci, F., et al. (2004). Phase II trial of the histone deacetylase inhibitor pivaloyloxymethyl butyrate (Pivanex, AN-9) in advanced non-small cell lung cancer. Lung Cancer *45*, 381–386.
19. Edelman, M.J., Bauer, K., Khanwani, S., Tait, N., Trepel, J., Karp, J., Nemieboka, N., Chung, E.-J., and Van Echo, D. (2003). Clinical and pharmacologic study of tributyrin: an oral butyrate prodrug. Cancer Chemother. Pharmacol. *51*, 439–444.
20. Böhmig, G.A., Krieger, P.-M., Säemann, M.D., Ullrich, R., Karimi, H., Wekerle, T., Mühlbacher, F., and Zlabinger, G.J. (1999). Stable prodrugs of *N*-butyric acid: suppression of T cell alloresponses in vitro and prolongation of heart allograft survival in a fully allogeneic rat strain combination. Transpl. Immunol. *7*, 221–227.
21. Pouillart, P., Ronco, G., Cerutti, I., Trouvin, J.H., Pieri, F., and Villa, P. (1992). Pharmacokinetic studies of *N*-butyric acid mono- and polyesters derived from monosaccharides. J. Pharm. Sci. *81*, 241–244.
22. Pouillart, P., Douillet, O., Scappini, B., Gozzini, A., Santini, V., Grossi, A., Pagliai, G., Strippoli, P., Rigacci, L., Ronco, G., et al. (1999). Regioselective synthesis and biological profiling of butyric and phenylalkylcarboxylic esters derivated from D-mannose and xylitol: influence of alkyl chain length on acute toxicity. Eur. J. Pharm. Sci. *7*, 93–106.
23. Corfield, A.P., Myerscough, N., Gough, M., Brockhausen, I., Schauer, R., and Paraskeva, C. (1995). Glycosylation patterns of mucins in colonic disease. Biochem. Soc. Trans. *23*, 840–845.
24. Sell, S. (1990). Cancer-associated carbohydrates identified by monoclonal antibodies. Hum. Pathol. *21*, 1003–1019.
25. Kobata, A., and Amano, J. (2005). Altered glycosylation of proteins produced by malignant cells, and application for the diagnosis and immunotherapy of tumours. Immunol. Cell Biol. *83*, 429–439.
26. Hadfield, A.F., Mella, S.L., and Sartorelli, A.C. (1983). *N*-acetyl-D-mannosamine analogues as potential inhibitors of sialic acid biosynthesis. J. Pharm. Sci. *72*, 748–751.
27. Deshpande, P.P., and Danishefsky, S.J. (1997). Total synthesis of the potential anticancer vaccine KH-1 adenocarcinoma antigen. Nature *387*, 164–166.
28. Krug, L.M. (2004). Vaccine therapy for small cell lung cancer. Semin. Oncol. *31*, 112–116.
29. Hakomori, S. (2001). Tumor-associated carbohydrate antigens defining tumor malignancy: basis for development of anti-cancer vaccines. Adv. Exp. Med. Biol. *491*, 369–402.
30. Chen, H., Wang, Z., Sun, Z., Kim, E.J., and Yarema, K.J. (2005). Mammalian glycosylation: an overview of carbohydrate biosynthesis. In Handbook of Carbohydrate Engineering., K.J. Yarema, ed. (Boca Raton, FL: Francis & Taylor/CRC Press), pp. 1–48.
31. Hanisch, F.G. (2001). *O*-glycosylation of the mucin type. Biol. Chem. *382*, 143–149.
32. Chou, T.Y., and Hart, G.W. (2001). *O*-linked *N*-acetylglucosamine and cancer: messages from the glycosylation of c-Myc. Adv. Exp. Med. Biol. *491*, 413–418.
33. Kim, Y.S., Gum, J., and Brockhausen, I. (1996). Mucin glycoproteins in neoplasia. Glycoconj. J. *13*, 693–707.
34. Hang, H.C., and Bertozzi, C.R. (2005). The chemistry and biology of mucin-type *O*-linked glycosylation. Bioorg. Med. Chem. *13*, 5021–5034.

35. Keppler, O.T., Horstkorte, R., Pawlita, M., Schmidt, C., and Reutter, W. (2001). Biochemical engineering of the *N*-acyl side chain of sialic acid: biological implications. Glycobiology *11*, 11R–18R.
36. Goon, S., and Bertozzi, C.R. (2002). Metabolic substrate engineering as a tool for glycobiology. J. Carbohydr. Chem. *21*, 943–977.
37. Jones, M.B., Teng, H., Rhee, J.K., Baskaran, G., Lahar, N., and Yarema, K.J. (2004). Characterization of the cellular uptake and metabolic conversion of acetylated *N*-acetylmannosamine (ManNAc) analogues to sialic acids. Biotechnol. Bioeng. *85*, 394–405.
38. Ghosh, P., Ender, I., and Hale, E.A. (1998). Long-term ethanol consumption selectively inpairs ganglioside pathway in rat brain. Alcohol. Clin. Exp. Res. *22*, 1220–1226.
39. Suzuki, O., Nozawa, Y., and Abe, M. (2003). Sialic acids linked to glycoconjugates of Fas regulate the caspase-9-dependent and mitochondria-mediated pathway of Fas-induced apoptosis in Jurkat T cell lymphoma. Int. J. Oncol. *23*, 769–774.
40. Eda, S., Yamanaka, M., and Beppu, M. (2004). Carbohydrate-mediated phagocytic recognition of early apoptotic cells undergoing transient capping of CD43 glycoprotein. J. Biol. Chem. *279*, 5967–5974.
41. Malisan, F., and Testi, R. (2002). GD3 in cellular ageing and apoptosis. Exp. Gerontol. *37*, 1273–1282.
42. Chen, H.Y., and Varki, A. (2002). O-acetylation of GD3: an enigmatic modification regulating apoptosis. J. Exp. Med. *196*, 1529–1533.
43. Malykh, Y.N., Schauer, R., and Shaw, L. (2001). *N*-glycolylneuraminic acid in human tumours. Biochimie *83*, 623–634.
44. Kim, E.J., Sampathkumar, S.-G., Jones, M.B., Rhee, J.K., Baskaran, G., and Yarema, K.J. (2004). Characterization of the metabolic flux and apoptotic effects of *O*-hydroxyl- and *N*-acetylmannosamine (ManNAc) analogs in Jurkat (human T-lymphoma-derived) cells. J. Biol. Chem. *279*, 18342–18352.
45. Zachara, N.E., O'Donnell, N., Cheung, W.D., Mercer, J.J., Marth, J.D., and Hart, G.W. (2004). Dynamic O-GlcNAc modification of nucleocytoplasmic proteins in response to stress: a survival response of mammalian cells. J. Biol. Chem. *279*, 30133–30142.
46. Fishman, P.H., and Brady, R.O. (1976). Biosynthesis and function of gangliosides. Science *194*, 906–915.
47. Sarkar, A.K., Fritz, T.A., Taylor, W.H., and Esko, J.D. (1995). Disaccharide uptake and priming in animal cells: inhibition of sialyl Lewis X by acetylated Gal β1,4GalcNAc β-*O*-naphthalenemethanol. Proc. Natl. Acad. Sci. USA *92*, 3323–3327.
48. Rosato, R.R., Almenara, J.A., Cartee, L., Betts, V., Chellappan, S.P., and Grant, S. (2002). The cyclin-dependent kinase inhibitor flavopiridol disrupts sodium butyrate-induced p21WAF1/CIP1 expression and maturation while reciprocally potentiating apoptosis in human leukemia cells. Mol. Cancer Ther. *1*, 253–266.
49. El-Deiry, W.S., Tokino, T., Velculescu, V.E., Levy, D.B., Parsons, R., Trent, J.M., Lin, D., Mercer, W.E., Kinzler, K.W., and Vogelstein, B. (1993). WAF1, a potential mediator of p53 tumor suppression. Cell *75*, 817–825.
50. Bai, L., and Merchant, J.L. (2000). Transcription factor ZBP-89 cooperates with histone acetyltransferase p300 during butyrate activation of p21(WAF1) transcription in human cells. J. Biol. Chem. *275*, 30725–30733.
51. Siddiqui, R.A., Jenski, L.J., Harvey, K.A., Wiesehan, J.D., Stillwell, W., and Zaloga, G.P. (2003). Cell-cycle arrest in Jurkat leukaemic cells: a possible role for docosahexaenoic acid. Biochem. J. *371*, 621–629.
52. Blagosklonny, M.V., Robey, R., Sackett, D.L., Du, L., Traganos, F., Darzynkiewicz, Z., Fojo, T., and Bates, S.E. (2002). Histone deacetylase inhibitors all induce p21 but differentially cause tubulin acetylation, mitotic arrest, and cytotoxicity. Mol. Cancer Ther. *2002*, 937–941.
53. Darzynkiewicz, Z., Juan, G., and Bedner, E. (1999). Determining cell cycle stages by flow cytometry. In Current Protocols in Cell Biology, J.S. Bonifacino, M. Dasso, and J.B. Harford, eds. (New York: John Wiley & Sons), pp. 8.4.1–8.4.18.
54. Kim, E.J., Jones, M.B., Rhee, J.K., Sampathkumar, S.-G., and Yarema, K.J. (2004). Establishment of *N*-acetylmannosamine (ManNAc) analogue-resistant cell lines as improved hosts for sialic acid engineering applications. Biotechnol. Prog. *20*, 1674–1682.
55. Dancey, J.E., and Chen, H.X. (2006). Strategies for optimizing combinations of molecularly targeted anticancer drugs. Nat. Rev. Drug Discov. *5*, 649–659.
56. Luchansky, S.J., Yarema, K.J., Takahashi, S., and Bertozzi, C.R. (2003). GlcNAc 2-epimerase can serve a catabolic role in sialic acid metabolism. J. Biol. Chem. *278*, 8036–8042.
57. Wang, Z., Sun, Z., Li, A.V., and Yarema, K.J. (2006). Roles for GNE outside of sialic acid biosynthesis: modulation of sialyltransferase and BiP expression, GM3 and GD3 biosynthesis, proliferation and apoptosis, and ERK1/2 phosphorylation. J. Biol. Chem. *281*, 27016–27028.
58. Hara, I., Miyake, H., Hara, S., Arakawa, S., and Kamidono, S. (2000). Sodium butyrate induces apoptosis in human renal cell carcinoma cells and synergistically enhances their sensitivity to anti-Fas-mediated cytotoxicity. Int. J. Oncol. *17*, 1213–1218.
59. Chopin, V., Slomianny, C., Hondermarck, H., and Le Bourhis, X. (2004). Synergistic induction of apoptosis in breast cancer cells by cotreatment with butyrate and TNF-alpha, TRAIL, or anti-Fas agonist antibody involves enhancement of death receptors' signaling and requires P21(waf1). Exp. Cell Res. *298*, 560–573.
60. Williams, E.A., Coxhead, J.M., and Mathers, J.C. (2003). Anticancer effects of butyrate: use of micro-array technology to investigate mechanisms. Proc. Nutr. Soc. *62*, 107–115.
61. Comelli, E.M., Head, S.R., Gilmartin, T., Whisenant, T., Haslam, S.M., North, S.J., Wong, N.-K., Kudo, T., Narimatsu, H., Esko, J.D., et al. (2006). A focused microarray approach to functional glycomics: transcriptional regulation of the glycome. Glycobiology *16*, 117–131.
62. Scheppach, W., and Weiler, F. (2004). The butyrate story: old wine in new bottles? Curr. Opin. Clin. Nutr. Metab. Care *7*, 563–567.
63. Jourdian, G.W., Dean, L., and Roseman, S. (1971). The sialic acids: XI. A periodate-resorcinol method for the quantitative estimation of free sialic acids and their glycosides. J. Biol. Chem. *246*, 430–435.